

Flavonoids from *Smilax china* L. Rhizome improve chronic pelvic inflammatory disease by promoting macrophage reprogramming via the NLRP3 inflammasome-autophagy pathway

Yun Ma ^a, Tingting Pei ^a, Luyao Song ^a, Daoqi Zhu ^a, Zhongxiao Han ^a, Jiaxing Zhang ^a, Xintao Huang ^a, Xinhuan Qiu ^a, Wei Xiao ^{b,*}

^a Department of Pharmacy, Clinical Pharmacy Center, Nanfang Hospital, Southern Medical University, Guangzhou, Guangdong, China

^b Key Laboratory of Gluclolipid Metabolic Disorder, Ministry of Education, Guangdong Pharmaceutical University, Guangzhou, Guangdong, China

ARTICLE INFO

Keywords:

Flavonoid extract of *Smilax china* L.
Chronic pelvic inflammation
Macrophage reprogramming
Inflammasome
Autophagy

ABSTRACT

Background: *Smilax* is a traditional medicine used for the clinical treatment of pelvic inflammatory disease (PID), and its leaves have long been used as food by the Korean people in Asia. In previous studies, we found that flavonoids extract can improve PID by inhibiting inflammation, which may be the main effective component of *Smilax China*, but its mechanism of action has not been fully elucidated. This study explores the mechanism by which Chinese rhizome flavonoids (FCSR) regulate the autophagy pathway of NLRP3 inflammasome and promote macrophage reprogramming.

Methods: In the *in vivo* experiment, the sham surgery group and the PID group were given physiological saline and FCSR for 7 days, respectively. We determined the expression of NLRP3 inflammasome autophagy pathway genes and proteins by observing the pathological damage of rat uteri through HE and Masson staining, immunofluorescence, RT-PCR, and WB experiments. Molecular docking simulation predicted the binding potential of flavonoids with the potential target VPS34, and knockdown experiments were conducted to validate the knockdown effect of lipopolysaccharide treatment on primary rat endometrial cells to simulate an *in vitro* PID model.

Results: FCSR significantly reduced serum IL-1 β in PID rats, TNF- α . The concentration of TAX2 reduced the infiltration of inflammatory cells and fibrosis of endometrial cells, promoted M2 polarization of macrophages, upregulated autophagy pathways, and inhibited the activation of NLRP3 inflammasomes. After knocking down the NLRP3 inflammasome autophagy target VPS34, the FCSR effect was eliminated.

Conclusions: By targeting VPS34, FCSR potentially promotes autophagic cell reprogramming through the NLRP3 inflammasome related autophagy pathway.

1. Introduction

Pelvic inflammatory disease (PID) is an inflammatory disease that is highly prevalent in sexually active women and is usually a consequence of upper reproductive tract infection (Curry, Williams, & Penny, 2019). Currently, approximately 4–12% of fertile women worldwide are affected by PID (Savaris, Fuhrich, Maissiat, Duarte, & Ross, 2020). PID can be classified into acute and chronic types. The duration of acute pelvic inflammatory disease (APID) is ≤ 30 days and is usually associated with cervical or vaginal microbes (including *Neisseria gonorrhoeae*

and *Chlamydia trachomatis*); chronic pelvic inflammatory disease (CPID) lasts for > 30 days; the common causative pathogens are *Mycobacterium tuberculosis* and *Actinomycetes* (Brunham, Gottlieb, & Paavonen, 2015). APID without thorough treatment may develop into CPID (Kou, Ding, Chen, Liu, & Liu, 2016; Y. Li et al., 2018). Chronic inflammation causes fallopian tube injury, pelvic adhesions, and fibrosis (Mitchell & Prabhu, 2013), which are key factors for the sequelae caused by female genital tract lesions (Zou et al., 2021). Currently, the primary clinical treatment for PID is antimicrobial therapy. Although antibacterial treatment improves microbial infection, it does not improve the inflammatory effects

* Corresponding author at: Key Laboratory of Gluclolipid Metabolic Disorder, Ministry of Education, Guangdong Pharmaceutical University, Guangzhou, Guangdong 510006, China.

E-mail address: xw7688@smu.edu.cn (W. Xiao).

of PID. Furthermore, prolonged antimicrobial therapy can cause widespread drug resistance (Costa-Lourenço, Barros Dos Santos, Moreira, Fracalanza, & Bonelli, 2017; Savaris et al., 2020) and can also affect the reproductive outcomes of patients receiving treatment (Brunham et al., 2015). In addition to antimicrobial therapy, nonsteroidal anti-inflammatory drugs (NSAIDs) are often used to treat PID in clinical practice. However, NSAIDs have limited efficacy and can cause many adverse reactions (Baron et al., 2013; Fan et al., 2014).

Due to the limitations of antibiotics, research is increasingly focusing on the role of natural products in the treatment of CPID. Studies have found that Penyanling granules inhibit the infiltration of lymphocytes and neutrophils in uterine tissue, improving PID through anti-inflammatory effects. Its effective ingredients include flavonoids, phenolics, and saponins (Zou et al., 2021); Fukeqianjin formula (including components from *Moghania macrophylla*, *Radix Rosa laevigata*, and *Andrographis paniculata*) has potential therapeutic effects on PID, which inhibits inflammation and improves metabolic disorders (Zhang et al., 2018c). Man-Pen-Fang is a traditional Chinese herbal compound, which is composed of *Thlaspi arvense* L., *Gleditsia sinensis* Lam., and *Smilax china* L., which also inhibits NF-κB for the treatment of CPID (L. J. Zhang et al., 2017). Additionally, in the studies of the effects of traditional Chinese medicine on CPID, Li et al. (2020) and Tang, Wu, Meng, and Wang (2019) found that inhibiting inflammatory factors may be the key to diminishing the impact of CPID. However, the lack of clarification on the transmission pathways and regulatory mechanisms of inflammatory signals is a common issue in current research. Therefore, it is imperative that we explore the pathogenesis of CPID and investigate the therapeutic effects of traditional drugs.

Although macrophages respond to pathogenic stimulation to inhibit the further development of inflammation and promote repair and healing of tissue wounds, they can also contribute to tissue damage during infection and inflammation (Shapouri-Moghaddam et al., 2018), and their role in inflammation depends on the polarization type. Macrophage polarization is mainly divided into the M1 and M2 types. M1 macrophages mediate ROS-induced tissue damage by releasing pro-inflammatory factors such as TNF-α, IL-1β, and IL-6, and impede tissue wound regeneration and healing. The release of anti-inflammatory factors such as IL-10 and transforming growth factor-β by M2 macrophages can promote tissue wound repair and healing by removing debris and apoptotic cells (Shapouri-Moghaddam et al., 2018). The polarization type of macrophages can be caused by local cytokines or environmental stimuli, usually manifesting as the early initiation of inflammation and the tendency of the M1 type to remove exogenous threats. In the later stages of inflammation, macrophages are polarized into M2 to control inflammation and promote tissue repair (Butenko et al., 2020), and the dynamic balance of M1/M2 polarization maintains immunity. Briefly, the initiation of inflammation is a protective measure by the body to defend against pathogen invasion, while a failed inflammatory response is the key factor that results in damage to the body (Nathan & Ding, 2010). Chronic inflammation can reactivate the recruitment of macrophages in a long-term and sustainable manner, and recruited macrophages tend to have M1 polarization (Alivernini et al., 2020). The M1 polarization of macrophages activates NLRP3 inflammasome (Zhang et al., 2020), which further drives the development of inflammation.

The NLRP3 inflammasome is a protein complex polymerized from the cytoplasm. Under stress, it in turn activates the inflammatory response, producing the inflammasome effector cytokines IL-1β and IL-18, and generating and maintaining the inflammatory microenvironment (Sharma & Kanneganti, 2021). Aberrantly activated NLRP3 leads to a chronic inflammatory state (Haneklaus & O'Neill, 2015), which is one of the main reasons for the poor prognosis observed in patients with pelvic inflammation. This confirms that the development of PIDs is closely associated with the NLRP3 inflammasome. However, previous studies have not clarified the changes and regulatory mechanisms of the NLRP3 inflammasome in CPID.

Autophagy is a very “conserved” process which allows for the

degradation of impaired organelles and abnormally deposited proteins by lysosomes. Although the regulation of autophagy in CPID has not been fully elucidated, it is interesting that decreased autophagy expression is closely associated with the failure of fertilization and embryo development (Tsukamoto et al., 2008). Activation of the NLRP3 inflammasome is a key step in triggering autophagy. Under physiological conditions, autophagy has been implicated in clearing the activated NLRP3 inflammasome and inhibiting the development of inflammation. In pathological states, autophagy dysfunction can reverse NLRP3 inflammasome hyperactivation (Haneklaus & O'Neill, 2015). However, the regulatory mechanism linking autophagy and NLRP3 inflammasomes in CPID remains unknown (Han et al., 2019).

Smilax china L. extract is obtained from the dry root of this Liliaceous plant. According to modern pharmacological research, *S. china* root extract has antibacterial, anti-inflammatory, anti-oxidative, anti-cancer, and other pharmacological activities (Hua et al., 2018), while its leaves are commonly used as food by Korean people in China. The total extract of *S. china* has been prepared as Jin Gang Teng capsules (No: Z20070006) and is marketed in China for the treatment of PID (Gao & Zhang, 2017), achieving a certain efficacy. Our previous study (Luyao, Liwen, Yun, & Feng, 2017) found that the total flavonoid extract from *S. china* has potent anti-inflammatory and antifibrotic efficacy in a rat model of PID; however, the mechanism underlying these beneficial effects are still unclear. The purpose of this study was to investigate the impact of *S. china* flavonoid extract on NLRP3 inflammasome-autophagy crosstalk, thus exploring the potential action mechanism of *S. china* in treating PID and facilitating the quest for drugs to treat CPID.

2. Materials and methods

2.1. Preparation of *Smilax china* L. Extracts

S. china was obtained from Anhui Run Furong Pharmaceutical Co., Ltd. (Bozhou, Anhui Province, China) in December 2019. The herb was identified via <https://www.theplantlist.org> and was confirmed by Professor Chuanning Liu of the China Department of Traditional Chinese Medicine, Southern Medical University. The specimens (*Smilax china* L. No. GCM-436) were stored at the Guangdong Key Laboratory of Traditional Chinese Medicine Preparations, Guangzhou, China.

The extract was prepared based on a previously reported extraction method (Song et al., 2017). First, 250 g of *S. china* was extracted with five times the volume of 95% ethanol for 1 h each in triplicate. The filtrate was then added and the mixture was concentrated to remove the alcohol. Next, 1250 mL of water was added (containing 0.2 g/mL raw medicinal materials), and the solution was filtered using an AB-8 (500 mL) macroporous resin. Elution was performed using eight times the volume of 40% ethanol, the mixture was concentrated, and 1000 mL of water was added. The suction filtrate was eluted with twice the volume of 20% ethanol using a filter column with polyamide mesh (80–100 mesh, 140 g). After concentration under reduced pressure, the samples were freeze-dried to obtain 0.9 g of extract. The flavonoid content in the extract was determined using UPLC (Song et al., 2017). The obtained extract was named as flavonoids from *S. china* rhizome (FSCR).

2.2. Preparation of phenol slurry

Simple optimization was carried out according to the preparation methods described in the literature. Briefly, 10 mL of glycerol (Hengjian, H44023815), 5 g of Huang yarrow gum (Zhejiang Yinnuo, 20211106), and 35 mL of phenol (Energy Chemical Industry, W610517) were mixed and ground to prepare a homogeneous phenol slurry.

2.3. Animals

Thirty female SD rats aged 10–12 weeks with a body weight of 200 ± 10 g were purchased from Hunan STJ Laboratory Animal Co., Ltd.

(Hunan, China), and were maintained in a specific pathogen-free (SPF) standard environment. The ambient temperature and humidity were stable at 25 ± 2 °C and $50 \pm 10\%$, respectively. All protocols complied with the Institutional Animal Care and Use Committee (IACUC) guidelines and were approved by the Animal Experiment Ethics Committee of South Medical University (Application No. NFYY-2019-0158).

2.4. Establishment of the CPID model and experimental design

Rats were randomly assigned to the following five groups: sham, CPID, FSCR-L, FSCR-M, and FSCR-H. After adaptive feeding for 1 week, all rats were operated on following inhalation anesthesia with isoflurane and deprived of food 12 h before the operation. In the sham group, 0.06 mL of normal saline was injected in the left uterus, and the other groups were injected with 0.06 mL of phenol slurry in the left uterus. After the operation, 10 mL of fluid (normal saline) was replenished. All animals woke up within 30 min of surgery, without abnormal behavior. Ten days after surgery, the sham and CPID groups were administered normal saline, FSCR-L (4.05 g·kg⁻¹), FSCR-M (8.1 g·kg⁻¹), and FSCR-H (16.2 g·kg⁻¹) intragastrically (i.g.). After 7 days of continuous administration, uterine tissue on the side of administration was collected. The experimental design is shown in Fig. 1A. The dosage of FSCR is typically calculated using the body surface area of rats and humans based on crude drugs and was calculated as such herein.

2.5. Morphological and histopathological examination

Uterine sections from each mouse were fixed with 4% phosphate-buffered saline (PBS)-buffered formaldehyde, then embedded in paraffin and finally cut to 5 μ m thickness for staining. Uterine sections were dewaxed using xylene, dehydrated by gradient ethanol, and finally stained with hematoxylin and eosin (H&E) and Masson's trichrome. All images were acquired using a Leica Laser Microcutting system (DM6B; Heidelberg, Germany).

2.6. Cell culture and treatment

Cell culture: Uterine tissue cut into small pieces was digested using collagenase (Sigma-Aldrich, C0130-1G, St. Louis, MO, USA) for a total of 2 h in an incubator with 37 °C. After centrifugation and washing,

complete medium (Procell, CM-R049, Wuhan, China) containing rat endometrial epithelial cells was added and left to stand for 4 h. The non-adherent cells were discarded to obtain the primary rat endometrial epithelial cells. The cells were cultured in complete media in a standard incubator with 37 °C at a 5% CO₂ atmosphere. Cell treatment: The cells were first inoculated on culture plates for 12 h, then treated with 1 μ g/mL LPS (Sigma-Aldrich, L2880) and LPS + FSCR (5, 10, 20 μ g/mL) for 24 h.

2.7. Cell viability assay

The cells were inoculated on 96-well plates (5×10^3 cells/well) for subsequent treatment. A CCK-8 kit (CELLCOOK, CT01A, Guangzhou, China) was used to measure cell viability. Cell viability was determined by measuring the absorbance at 450 nm using a microplate reader (Thermo, MULTISKAN MK3, Waltham, MA, USA).

2.8. Rhodamine staining

Rhodamine 123 (Beyotime, C2007, Shanghai, China) was used to assess mitochondrial function. After treatment, the medium was discarded and incubated with 10 μ M rhodamine-123 dye for 30 min. Then, after the media were discarded, the cells were fixed using 4% paraformaldehyde (Servicebio, G1101, Wuhan, China) for 15 min, and the nuclei were incubated with DAPI (Solarbio, C0065, Beijing, China) for 5 min. After staining, cells were photographed using a fluorescence microscope (Olympus, IX73 + DP73, Tokyo, Japan). The staining process is carried out with 37 °C.

2.9. Detection of apoptosis

The Beyotime One-step TUNEL Apoptosis Assay Kit (Red Fluorescence, Beyotime, C1090, Shanghai, China) was used to detect apoptosis. After treatment with the different drugs, the cells were stained in accordance with the manufacturer's instructions. After staining, cells were photographed using a fluorescence microscope (Olympus, IX73 + DP73).

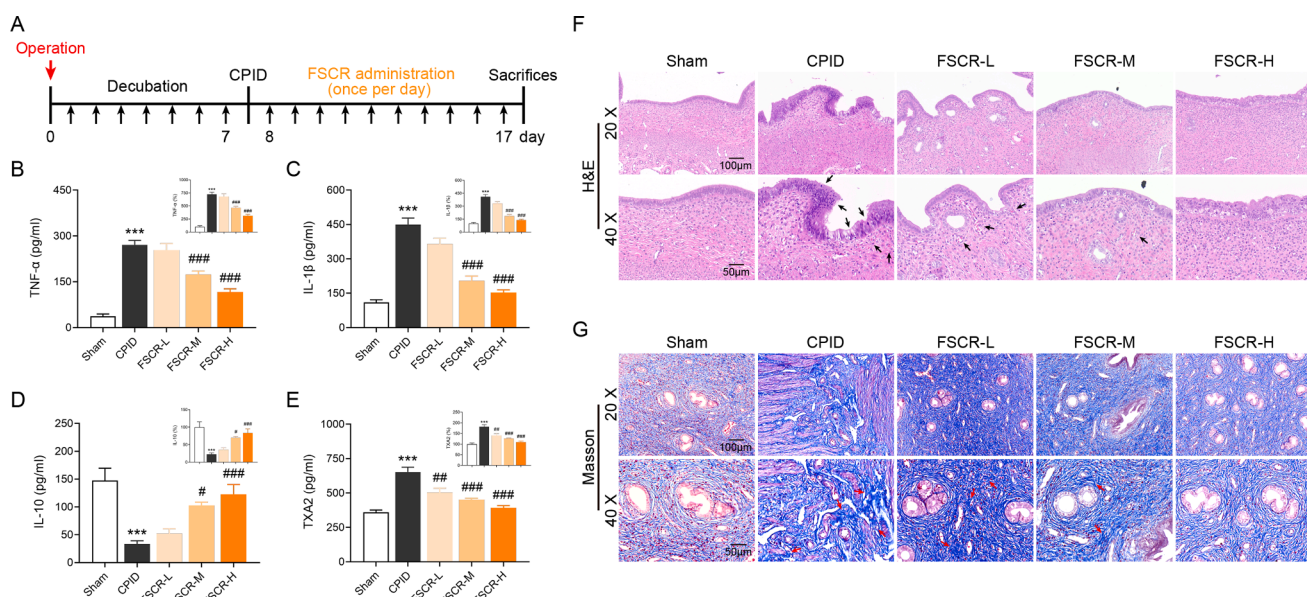


Fig. 1. FSCR improved CPID induced by phenol mucilage in rats. Schedule of the *in vivo* experimental design (A). Detection of serum cytokine concentrations in rats by ELISA: TNF- α (B), IL-1 β (C), IL-10 (D), and TXA2 (E). Histological changes and inflammatory cell infiltration (F) were observed by H&E staining. Masson staining was used to observe collagen proliferation and fibrosis (G). Results are presented as the mean \pm S.E.M. *** P < 0.001 vs. Sham; $^{\#}$ P < 0.05, $^{###}$ P < 0.001 vs. CPID.

2.10. Virus transfection

The vacuolar protein sorting 34 (VPS34) inflammasome was knocked down using a lentivirus transfection kit (GeneCopoeia, HSH104553, Guangzhou, China) in accordance with the manufacturer's instructions. The knockdown efficiency was verified using western blotting. Then, the Medium, LPS (1 μ g/mL), Sh-VPS343, FSCR (20 μ g/mL), and Sh-NLRP3 + FSCR groups were established, and the supernatants of cells were then aspirated after 24 h of LPS-induced inflammation.

2.11. ELISA

The concentrations of TNF- α , IL-1 β , and IL-10 in rat serum samples were confirmed by specific ELISA kits purchased from Multi Sciences (Lianke) Biotech, Co., Ltd. (Hangzhou, China). The concentration of TXA₂ was also determined, and the TXA₂ ELISA kit for rats (MM-0708R2) was purchased from Jiangsu Meimian Industrial Co., Jiangsu, China.

2.12. Immunofluorescence analysis

Paraffin-embedded sections of rat endometrial tissue (5 μ m) and primary rat endometrial epithelial cells were hybridized with the corresponding antibody. The antibodies used were anti-NLRP3, anti-VPS34 (1:500, 1:200 BF8029, DF8306; Affinity Biosciences Ltd.), anti-CD86, and anti-CD206 (1:200, 1:200, sc-19617, sc-58986; Santa Cruz Biotechnology, Inc.). After washing, the cells were combined with the corresponding IgG at 20–25 °C for 1 h. Nuclei were incubated with DAPI (C0065; Solarbio Science & Technology Co., Ltd.) at 20–25 °C for 6–8 min. Images were acquired using confocal microscopy (NI-U and DS-Ri2; Nikon, Tokyo, Japan).

2.13. RT-PCR analysis

RNA was extracted from rat endometrial tissues with Trizol reagent (absin), and cDNA was synthesized using the reverse transcriptase system (SureScriptTM First-Strand cDNA Synthesis Kit; GeneCopoeia, Guangzhou, China). Real-time PCR was used to validate the gene expression (SYBR; GeneCopoeia). The expression levels of all genes were normalized using the *ACTB* gene, and the $2^{-\Delta\Delta CT}$ method was used to calculate the relative gene expression. The primer sequences used for RT-PCR were acquired by Bio-Rad (CFX Connect) and synthesized by Sangon Biotech (Shanghai, China). These sequences are listed in Table 1.

2.14. Western blot analysis

Cultured primary rat endometrial epithelial cells and rat endometrial

Table 1
Real-time PCR primer sequences.

Target gene	Direction	Sequence
<i>CD86</i>	Forward primer	GGGCCATGCTCTCTTG
	Reverse primer	GATTGTCGTCCTGGGTA
<i>CD206</i>	Forward primer	CTCTGGACTCTGGATTGGA
	Reverse primer	TGATGATGGACTTCTGGT
<i>NLRP3</i>	Forward primer	TGTTGTCAGGATCTCGCA
	Reverse primer	AGTGAAGTAAGGCCGGAAT
<i>Caspase-1</i>	Forward primer	CAGATGCCAACACTGAA
	Reverse primer	CATGATCCCAACACAGGT
<i>ASC</i>	Forward primer	TGAAAACCTTGACAGCGGAT
	Reverse primer	GCCATACCCCTCCAGATAG
<i>IL-1β</i>	Forward primer	ATGGTCGGGACATAGTTGA
	Reverse primer	CTTGGCAGAGGACAAAGG
<i>IL-18</i>	Forward primer	AACGAATCCCGACAGACAG
	Reverse primer	AGAGGGTAGACATCCTCCAT
<i>ACTB</i>	Forward primer	CCTGGCACCCAGCACAAAT
	Reverse primer	GGGCCGGAATCGTCATAC

tissues were lysed for protein extraction using radioimmunoprecipitation assay (RIPA) lysis buffer with phenyl methyl sulfonyl fluoride (PMSF) solution, and the concentrations were detected using the BCA Protein Assay Kit (KeyGEN Biotech, Nanjing, China). Protein samples were electrophoretically separated on SDS-PAGE gels and electro-transferred onto PVDF membranes (Millipore, Burlington, MA, USA). The membranes were then incubated with the following primary antibodies: anti- β -actin, anti-NLRP3, anti-Caspase-1, anti-Cleaved-IL-1 β (1:6,000, 1:500, 1:1,000, 1:1,000, T0022-HRP, BF8029, AF5418, AF4006; Affinity Biosciences Ltd., Melbourne, VIC, Australia), anti-LAMP2, anti-Beclin1, anti-vps34, anti-p-vps34, anti-p62 (1:500, 1:1,000, 1:500, 1:500, 1:1,000, DF6719, AF5128, DF8306, AF7421, AF5384; Affinity Biosciences Ltd.), anti-CD86, anti-CD206 (1:500, 1:200, sc-19617, sc-58986; Santa Cruz Biotechnology, Inc., Dallas, TX, USA), and anti-LC3II (1:1,500, 12741S; Cell Signaling Technology, Inc., Danvers, MA, USA). The membranes were then co-incubated with a secondary antibody (1:10,000, Affinity Biosciences Ltd.). Finally, the stripe of each antibody was visualized and analyzed by ECL Reagent (Affinity Biosciences Ltd.) and ImageJ software.

2.15. Statistical analysis

The data are presented as mean \pm standard error (SEM) and were analyzed by GraphPad Prism 8.0.1. Among group variables were compared using one-way analysis of variance (ANOVA), followed by Tukey's post hoc tests ($P < 0.05$ indicated that the difference was statistically significant).

3. Results

3.1. FSCR regulates the abnormality of serum inflammatory factors and inhibits the infiltration of inflammatory cell and collagen fiber proliferation in the uteri of rats with CPID

The effects of FSCR on serum inflammatory factors, including TNF- α (Fig. 1B), IL-1 β (Fig. 1C), IL-10 (Fig. 1D), and TXA₂ (Fig. 1E), were determined by ELISA. These results suggest that rats with CPID were in a systemic inflammatory state. Plasma levels of TNF- α and IL-1 β were significantly increased, and IL-10 was significantly decreased in these animals relative to the control rats. FSCR significantly reduced plasma levels of TNF- α and IL-1 β and restored IL-10 release in rats with CPID, indicating that FSCR could correct the inflammatory state of rats with CPID in a dose-dependent manner. In addition, FSCR dose-dependently inhibited the increase in TXA₂ in rats with CPID, suggesting that FSCR could inhibit collagen hyperplasia and fibrosis in the uterine tissue of the animals.

Pathological observation is a key indicator for the diagnosis and treatment of CPID. H&E and Masson's staining were used to detect pathological changes in the endometria of rats. H&E staining showed that the CPID model group had obvious infiltration of inflammatory cells and abnormal morphology in the endometria relative to the sham group, and the administration of FSCR attenuated the pathological changes (Fig. 1F), suggesting that FSCR improved the inflammatory pathological damage to the endometria in rats with CPID. FSCR inhibited CPID-induced uterine collagen hyperplasia and fibrosis, which was observed by Masson staining (Fig. 1G).

3.2. FSCR promotes macrophage reprogramming in the uterine tissue of rats with CPID

Macrophage polarization is often used to study changes in the local immune micro-environment during inflammatory diseases. In this study, we examined the effect of FCSR on uterine macrophage polarization in rats with CPID by immunofluorescence (IF) using red-labeled CD86 (macrophage M1 polarization) and green-labeled CD206 (macrophage M2 polarization). In the IF observation of the sham group, it was found

that CD206 and CD86 were relatively balanced, and two polarization states of macrophages were observed simultaneously in the tissue (yellow observed by IF). CD86 expression was higher in the uteri of rats with CPID than in the sham group, consistent with macrophage recruitment and M1 polarization. The up-regulation of CD206 expression after FSCR administration suggests that the uterine macrophages became polarized toward the M2 type under the influence of FSCR in rats with CPID, restoring the balance of M1 and M2 polarization through macrophage reprogramming (Fig. 2A).

The expressions of CD86 (Fig. 2B), CD163 (Fig. 2C), and CD206 (Fig. 2D) were determined at the mRNA and protein levels, respectively (Fig. 2E). As with the IF results, CD86 expression was upregulated and CD206 was downregulated in the CPID group. The administration of FSCR inhibited the macrophage polarization imbalance in a dose-dependent manner, suggesting that FSCR promoted macrophage reprogramming in the uterine tissue of rats with CPID.

3.3. FSCR inhibits the activation of the NLRP3 inflammasome-autophagy pathway in the uteri of rats with CPID

The change in macrophage polarization is an important factor in the activation of NLRP3 inflammasome in the innate immune system. RT-PCR suggested that the mRNA expression of *NLRP3*, *CASP1*, *ASC*, *IL-1 β* , and *IL-18* were all up-regulated in the CPID group (Fig. 3A), and the transcription of NLRP3 inflammasome components and effectors was down-regulated in a dose-dependent manner following FSCR administration. This suggests that FSCR inhibits NLRP3 inflammasome initiation to a certain extent. Western blotting showed that FSCR inhibited NLRP3, and cleaved-CASP1 and cleaved-IL-1 β were up-regulated, further suggesting that FSCR suppressed the activation of NLRP3 inflammasome.

Autophagy acts as one of the key factors regulating the NLRP3 inflammasome. The changes in the autophagic pathway were detected by western blot assay (Fig. 3C). CPID inhibited autophagy by down-regulating the expression of *p*-VPS34. FSCR dose-dependently up-regulated Beclin 1 and *p*-VPS34, while decreasing the autophagy substrate p62, suggesting that FSCR restored the inhibited autophagy pathway.

IF was used to study the localization of NLRP3 inflammasomes and autophagosomes in the uterine tissues of rats. The NLRP3 inflammasome was observed by labeling NLRP3 with red fluorescence, and autophagic vesicles were observed by labeling VPS34 with green fluorescence. The location of NLRP3 inflammasome and VPS34 were observed in tissues by merging different fluorescence colors. Compared with those in the sham group, the expression levels of NLRP3 in the CPID group was relatively increased and it was not observed to be located with VPS34. FSCR suppressed the expression of NLRP3 and up-regulated the expression of

VPS34, and both showed co-localization (yellow observed using IF) (Fig. 3D). These results suggest that FSCR promotes the interaction between autophagy and the NLRP3 inflammasome. The level of ubiquitination in the lysosomal pathway was investigated by western blot. As shown in Fig. 3E, LC3 II, LAMP2 (a key protein in the lysosomal pathway), and ubiquitin (a marker indicating ubiquitin degradation) were significantly down-regulated in the CPID group, and FSCR was dose-dependently up-regulated the expression of these proteins. These results suggest that FSCR restores the dysfunction of the autophagy-lysosome pathway caused by CPID and degrades the NLRP3 inflammasome by promoting the ubiquitination of autophagy lysosomes.

3.4. FSCR inhibits the LPS-induced CPID *in vitro* model from primary rat endometrial cells

An *in vitro* model was used to verify the mechanism underlying the beneficial effects of FSCR in CPID. Primary rat endometrial cells were isolated, cultured, and stimulated with LPS to simulate CPID in an *in vitro* model. ELISA results showed that FSCR significantly suppressed IL-1 β (Fig. 4A) and IL-18 (Fig. 4B) induced by LPS in the supernatant of the cells.

Similar to the results of the *in vivo* assays, NLRP3 expression was up-regulated after LPS (1 μ g/mL) stimulation, and FSCR was administered to suppress the expression of NLRP3 and promote VPS34 expression. Co-localization of NLRP3 and VPS34 was observed (yellow fluorescence) in primary rat endometrial cell lines (Fig. 4C).

As determined by TUNEL staining, compared to the rate of apoptosis in the medium group, the LPS group showed increased apoptosis (red fluorescence). Additionally, FSCR inhibited the apoptosis of primary rat endometrial epithelial cells in a dose-dependent manner (Fig. 4D).

The protein expression level of NLRP3 and *p*-VPS34 were investigated by western blot. *p*-VPS34 were significantly down-regulated in the CPID group, while NLRP3 were significantly up-regulated. FSCR dose-dependently recovered the expression of these proteins (Fig. 4E).

3.5. VPS34 is a potential target for FSCR to improve CPID

Molecular docking was used to predict the possible targets of FSCR. Previous studies have indicated that FSCR contains five flavonoids: astilbin, emgelitin, isoastilbin, isoengeletin, and quercetin 3-O- α -L-arabinopyranoside. The binding of these molecules was simulated with NLRP3, the key protein of the NLRP3 inflammasome, and VPS34, a key protein in the autophagy pathway. All five compounds showed good interaction potential with VPS34 (Fig. 5A). sh-vps34 coated with AAV was used to knockdown VPS34 in rat primary uterine epithelial cells (see

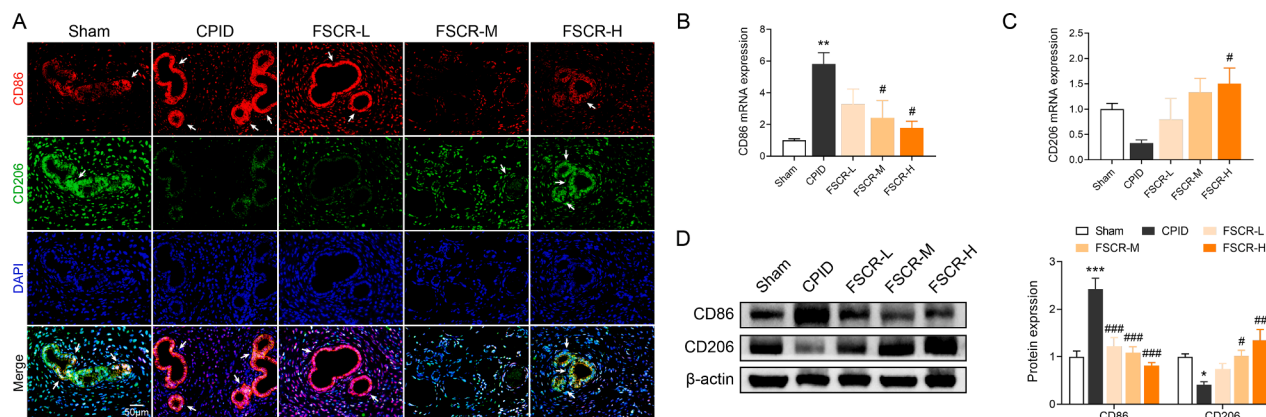


Fig. 2. Effect of FSCR on macrophage polarization in a rat model of CPID. Polarization markers were detected in uterine tissue by IF. CD86 was labeled with red fluorescence, CD206 was labeled with green fluorescence, and nuclei were labeled with DAPI (A). CD86 (B) and CD206 (C) were detected by RT-PCR. Protein levels of CD86 and CD206 were detected by western blotting (D). Results are presented as the mean \pm S.E.M. * P $<$ 0.05, ** P $<$ 0.01, *** P $<$ 0.001 vs. Sham; # P $<$ 0.05, # P $<$ 0.01, ### P $<$ 0.001 vs. CPID.

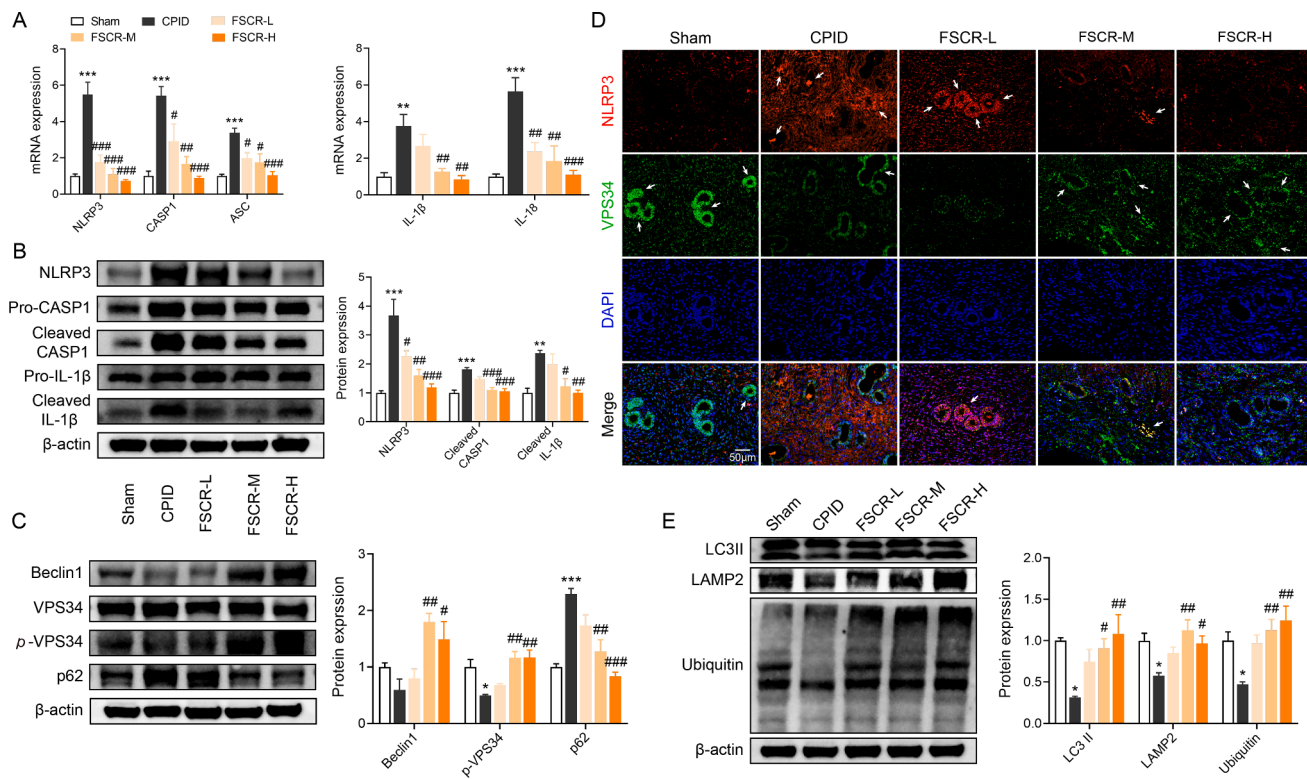


Fig. 3. Effect of FSCR on the NLRP3 inflammasome-related autophagy signaling pathway in uterine tissue of CPID rats. Detection of mRNA expression in NLRP3 inflammatory bodies by RT-PCR: *NLRP3*, *CASP1*, *ASC*, *IL-1 β* , and *IL-18* (A). Western blot detection of proteins in the NLRP3 inflammatory body: NLRP3, cleaved-CASP1, and cleaved-IL-1 β (B). Western blot detection of proteins in the autophagy pathway: Beclin1, p-VPS34, and p62 (C). The expression of NLRP3 inflammatory bodies and autophagic vesicles in uterine tissues was observed by IF: NLRP3 was labeled with red fluorescence, VPS34 was labeled with green fluorescence, and nuclei were labeled with DAPI with blue fluorescence (D). Western blot detection of proteins in the lysosomal pathway: LAMP2, Ubiquitin and LC3 II (E). Results are presented as the mean \pm S.E.M. *P < 0.05, **P < 0.01, ***P < 0.001 vs. Sham; #P < 0.05, ##P < 0.01, ###P < 0.001 vs. CPID.

Fig. 5B for a schematic diagram). IF verified the efficiency of sh-vps34 (Fig. 5C). The knockdown efficiency was 84.5%, as determined by western blotting (Fig. 5D), with no effects on the concentrations of IL-1 β and IL-18 (Fig. 5E), suggesting that the knockdown was acceptable for subsequent experiments. The detection of IL-18 (Fig. 5F) and IL-1 β (Fig. 5G) in cell supernatants after LPS administration showed that the effect of FSCR in inhibiting inflammatory factor release was significantly reduced after knocking down VPS34, indicating that VPS34 is a potential target for FSCR.

4. Discussion

This study reported an improvement in rats with CPID after treatment with FSCR. Briefly, FSCR inhibited activation of NLRP3 inflammasome and degraded the expression by driving autophagy, which subsequently promotes reprogramming of macrophages. FSCR can improve CPID in a dose-dependent manner, reducing the serum inflammatory factor content and weakening the infiltration of uterine inflammatory cells in a rat model. The results of this study showed that FSCR markedly improves CPID in rats and that NLRP3 may be one of its key sites of action.

In this study, the CPID model was established by chemical burn (injection of phenol glue) to simulate inflammation caused by non-infectious factors (Zhang et al., 2018). The vast majority (>90%) of patients with clinical infection-induced PID continue to develop CPID even after receiving the recommended treatment regimen (Brunham et al., 2015). The results of this study and previous studies show that non-infectious pathogenic factors also lead to the release of plasma pro-inflammatory factors (TNF- α and IL-1 β) in model animals, and these factors exert an enormous function on inflammation (Zhang et al.,

2018). However, the decreased concentration of the anti-inflammatory factor IL-10 suggests that the inflammatory response mediating cellular immune function is enhanced (Wen et al., 2020). In the model group, FSCR significantly improved the inflammatory response in rats with CPID in a dose-dependent manner.

Inflammation and its complications are the focus of most recent studies of CPID. However, changes in the immune microenvironment may be key factors that drive the local inflammatory response in the uterus (Sevostyanova et al., 2020). Our findings showed that FCSR suppressed the infiltration of inflammatory cells and monocytes into the endometrium of rats with CPID. Local inflammation can recruit circulating monocytes to tissues, and the monocytes can differentiate into macrophages when stimulated by pro-inflammatory factors (Jović, Kosač, & Koprivsek, 2014). The local cytokine environment can also polarize macrophages into two phenotypes: classical activation/inflammation (M1) and substitution activation/anti-inflammatory (M2) (Martinez & Gordon, 2014). Recent research on CPID has focused on the immune responses of macrophages and T cells (Z. Zhang, Zhang, & Zhang, 2022). Our results also showed that endometrial macrophages of rats with CPID had obvious M1-type polarization, and driven by FCSR, macrophages could transform to the M2-type. This suggests that FCSR promotes macrophage reprogramming, which may be an important factor in improving CPID.

The NLRP3 inflammasome exerts a significant function on the M1-type polarization of macrophages, driving chronic inflammatory responses by secreting mature IL-18 and IL-1 β (Lima-Junior, Mineo, Calich, & Zamboni, 2017). The results showed that the expression of the assembly elements of the NLRP3 inflammasome in the uterus of rats with CPID was upregulated and activation was increased, and these effects were inhibited by FSCR. By investigating the role of autophagy, the

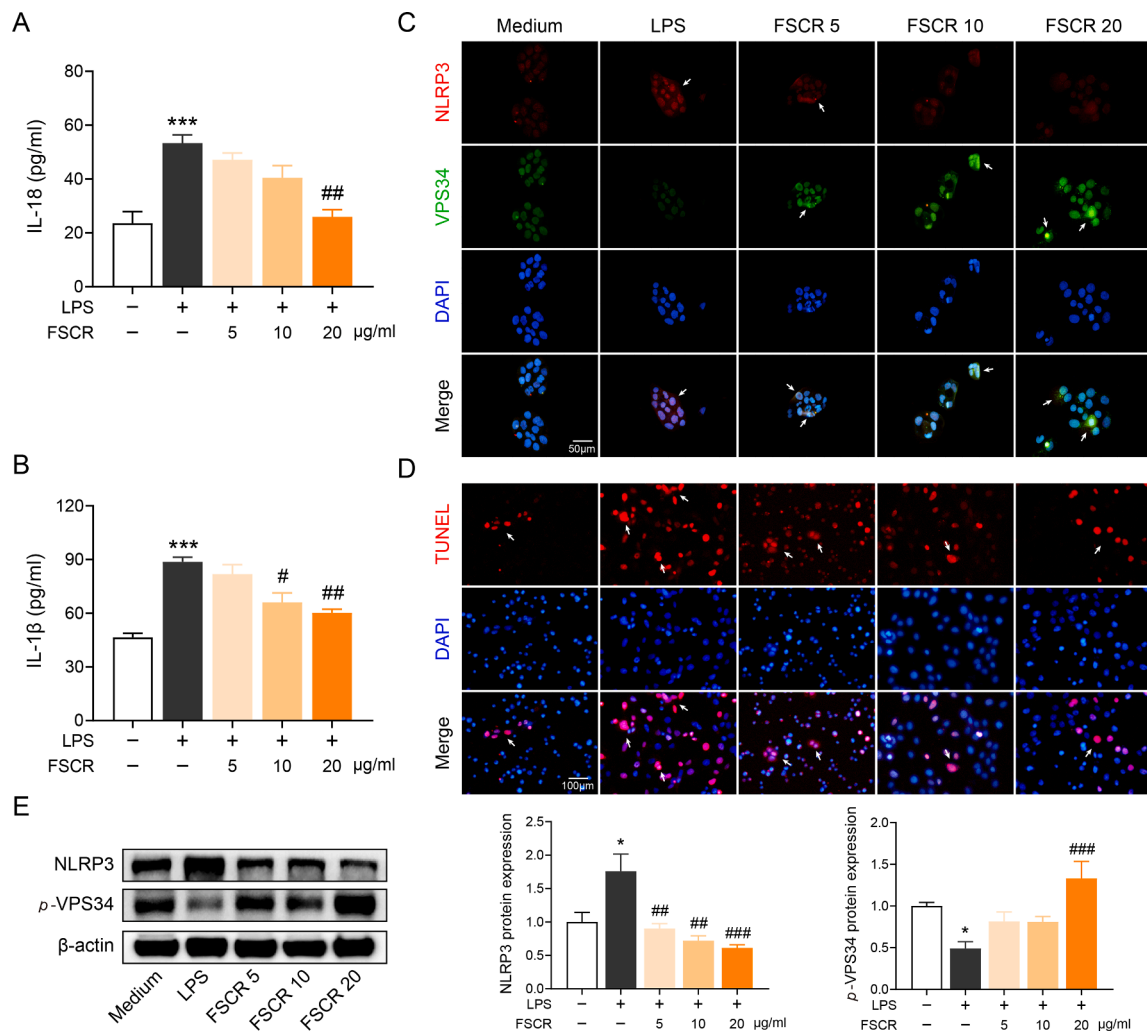


Fig. 4. Effect of FSCR on LPS-stimulated primary rat endometrial cells. Detection of IL-18 (A) and IL-1 (B) in the cell supernatant after FSCR and LPS stimulation, as determined by ELISA. IF demonstrated the expression of markers of NLRP3 inflammatory bodies and autophagic vesicles: NLRP3 was labeled with red fluorescence, VPS34 was labeled with green fluorescence, and the nuclei were labeled with DAPI in blue (C). IF observation of cell apoptosis: apoptotic bodies are marked by TUNEL in red, and nuclei are marked by DAPI in blue (D). Protein expression of NLRP3 and p-VPS34 by western blot (E). Results are presented as the mean \pm S.E.M. * P < 0.05, ** P < 0.01, *** P < 0.001 vs. Medium; # P < 0.05, ## P < 0.01, ### P < 0.001 vs. LPS.

pathway was explored by which FSCR suppressed the NLRP3 inflammasome. Autophagy clears abnormal proteins and organelles of pathogens via degradation pathways and has a hand in the regulation of NLRP3 in a variety of chronic inflammatory diseases (Ornatowski et al., 2020; Saitoh & Akira, 2016). After FSCR administration, autophagy was inhibited in CPID, the autophagy-lysosomal pathway was activated, and ubiquitination degradation increased. The IF results further confirmed that FSCR drives autophagy to mediate the degradation of the NLRP3 inflammasome, suggesting that autophagy is the key factor in improving CPID.

Previous studies have shown that FSCR contains five main flavonoid components (Song et al., 2017). Through molecular docking, their interaction with key molecules in the NLRP3 inflammasome autophagy pathway was simulated, and all these molecules had high scores with VPS34. These findings suggest that VPS34 exerts a significant function on the autophagy-promoting effect of FSCR. Therefore, we knocked down VPS34 using AAV to investigate the effect of the intervention on FSCR. After knocking down VPS34 at the cellular level, the effect of FSCR in inhibiting inflammatory factor release was significantly reduced, further suggesting that VPS34 is a key target of FSCR. Although this study yielded promising results, many questions still need to be addressed to understand the effects of *S. china* L. and its extracts on

CPID. For example, do multiple active ingredients act synergistically or does a certain component or metabolite play a dominant role in the improvement of CPID? At which concentration is the therapeutic effect of FSCR best in CPID? These issues should be the focus of further research on the mechanism of action of *S. china* L. and optimizing pharmacological effects in CPID. In conclusion, FSCR has great effects on ameliorating CPID by promoting the phosphorylation of VPS34 to drive the degradation of the NLRP3 inflammasome through the autophagy-lysosomal pathway and by promoting the reprogramming of macrophages.

5. Conclusions

FCSR regulated inflammation, potentially targeting VPS34, and promotes autophagic cell reprogramming via the NLRP3 inflammasome-related autophagy pathway.

Funding

This research is supported by the National Natural Science Foundation of China (No. 81873332).

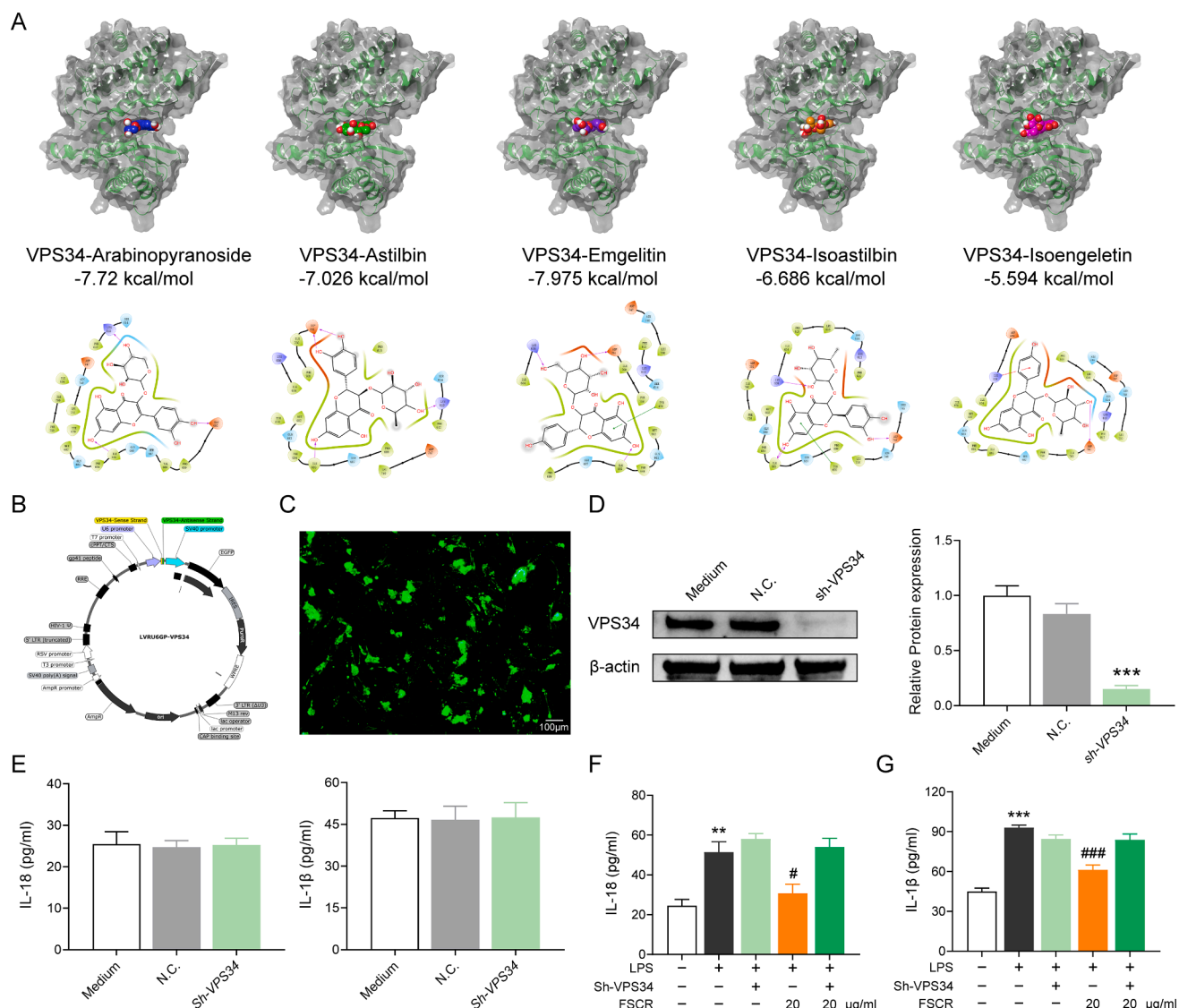


Fig. 5. Knock down of VPS34 and the effect of FSCR on CPID. Molecular docking simulation (A) of the five main flavonoids of FSCR on VPS34. Schematic diagram of VPS34 shRNA encapsulated by AAV (B). IF was used to observe the transfection efficiency (C). Western blot assay to verify the cell knockdown efficiency (D). Detection of IL-18 and IL-1 β (E) in the supernatant of cells transfected with VPS34 shRNA by ELISA. Detection of IL-18 and IL-1 β in primary rat endometrial cells induced by LPS (F). Results are presented as the mean \pm S.E.M. ** P < 0.01, *** P < 0.001 vs. Medium; # P < 0.05, ## P < 0.001 vs. LPS.

Ethics Statement

We conducted all animal experiments according to the National Research Council's Guide for the Care and Use of Laboratory Animals guidelines and were approved by the Animal Experiment Ethics Committee of South Medical University (Application No. NFYY-2019-0158).

CRediT authorship contribution statement

Yun Ma: Writing – review & editing, Writing – original draft, Funding acquisition, Conceptualization. **Tingting Pei:** Writing – original draft, Visualization, Methodology. **Luyao Song:** Visualization, Methodology. **Daoqi Zhu:** Software, Formal analysis, Data curation. **Zhongxiao Han:** Formal analysis, Data curation. **Jiaxing Zhang:** Visualization, Supervision. **Xintao Huang:** Validation. **Xinhuan Qiu:** Validation. **Wei Xiao:** Writing – review & editing, Supervision, Conceptualization.

Declaration of Competing Interest

The authors declare that they have no known competing financial interests or personal relationships that could have appeared to influence the work reported in this paper.

Data availability

Data will be made available on request.

Acknowledgments

We wish to thank Editage Insights Ltd. for timely help with language touchups.

References

Alivernini, S., MacDonald, L., Elmesmari, A., Finlay, S., Tolusso, B., Gigante, M. R., ... Kurowska-Stolarska, M. (2020). Distinct synovial tissue macrophage subsets regulate inflammation and remission in rheumatoid arthritis. *Nature Medicine*, 26(8), 1295–1306. <https://doi.org/10.1038/s41591-020-0939-8>

Baron, J. A., Senn, S., Voelker, M., Lanas, A., Laurora, I., Thielemann, W., ... McCarthy, D. (2013). Gastrointestinal adverse effects of short-term aspirin use: A meta-analysis of published randomized controlled trials. *Drugs R D*, 13(1), 9–16. <https://doi.org/10.1007/s40268-013-0011-y>

Brunham, R. C., Gottlieb, S. L., & Paavonen, J. (2015). Pelvic inflammatory disease. *The New England Journal of Medicine*, 372(21), 2039–2048. <https://doi.org/10.1056/NEJMra1411426>

Butenko, S., Satyanarayanan, S. K., Assi, S., Schif-Zuck, S., Sher, N., & Ariel, A. (2020). Transcriptomic analysis of Monocyte-Derived Non-Phagocytic macrophages favors a role in limiting tissue repair and fibrosis. *Frontiers in Immunology*, 11, 405. <https://doi.org/10.3389/fimmu.2020.00405>

Costa-Loureço, A., Barros Dos Santos, K. T., Moreira, B. M., Fracalanza, S. E. L., & Bonelli, R. R. (2017). antimicrobial resistance in neisseria gonorrhoeae: History, molecular mechanisms and epidemiological aspects of an emerging global threat. *Brazilian Journal of Microbiology*, 48(4), 617–628. <https://doi.org/10.1016/j.bjm.2017.06.001>

Curry, A., Williams, T., & Penny, M. L. (2019). Pelvic inflammatory disease: Diagnosis, management, and prevention. *American Family Physician*, 100(6), 357–364.

Fan, L. L., Yu, W. H., Liu, X. Q., Cui, Z., Ma, J., & Li, C. P. (2014). A meta-analysis on effectiveness of acupuncture and moxibustion for chronic pelvic inflammatory disease. *Zhen Ci Yan Jiu*, 39(2), 156–163.

Gao, S., & Zhang, Q. (2017). Curative effect of jin'gangteng capsule combined with kangfuxiaoyao suppository in the treatment of chronic pelvic inflammatory disease. *Pakistan Journal of Pharmaceutical Sciences*, 30(5(Supplementary)), 1943–1946.

Han, X., Sun, S., Sun, Y., Song, Q., Zhu, J., Song, N., ... Hu, G. (2019). Small molecule-driven NLRP3 inflammation inhibition via interplay between ubiquitination and autophagy: Implications for parkinson disease. *Autophagy*, 15(11), 1860–1881. <https://doi.org/10.1080/15548627.2019.1596481>

Haneklaus, M., & O'Neill, L. A. (2015). NLRP3 at the interface of metabolism and inflammation. *Immunological Reviews*, 265(1), 53–62. <https://doi.org/10.1111/imr.12285>

Hua, S., Zhang, Y., Liu, J., Dong, L., Huang, J., Lin, D., & Fu, X. (2018). Ethnomedicine, phytochemistry and pharmacology of smilax glabra: An important traditional chinese medicine. *The American Journal of Chinese Medicine*, 46(2), 261–297. <https://doi.org/10.1142/s0192415x18500143>

Jović, N. J., Kosac, A., & Koprivsek, K. (2014). L-2-Hydroxyglutaric aciduria: A case report. *Srpski Arhiv za Celokupno Lekarstvo*, 142(5–6), 337–341. <https://doi.org/10.2298/sarh1406337j>

Kou, M. J., Ding, X. F., Chen, J. X., Liu, Y., & Liu, Y. Y. (2016). Traditional chinese medicine combined with hormone therapy to treat premature ovarian failure: A meta-analysis of randomized controlled trials. *African Journal of Traditional, Complementary, and Alternative Medicines*, 13(5), 160–169. <https://doi.org/10.21010/ajtcam.v13i5.21>

Li, X. H., Liu, Y. R., Jiang, D. H., Tang, Z. S., Qian, D. W., Song, Z. X., ... Chang, A. B. (2020). Research on the mechanism of chinese herbal medicine radix paeoniae rubra in improving chronic pelvic inflammation disease by regulating PTGS2 in the arachidonic acid pathway. *Biomedicine & Pharmacotherapy*, 129, Article 110052. <https://doi.org/10.1016/j.biopha.2020.110052>

Li, Y., Liu, Y., Yang, Q., Shi, Z., Xie, Y., & Wang, S. (2018). Anti-Inflammatory effect of feiyangchangweiyan capsule on rat pelvic inflammatory disease through JNK/NF- κ B pathway. *Evidence-based Complementary and Alternative Medicine*, 2018, 8476147. <https://doi.org/10.1155/2018/8476147>

Lima-Junior, D. S., Mineo, T. W. P., Calich, V. L. G., & Zamboni, D. S. (2017). Dectin-1 activation during leishmania amazonensis phagocytosis prompts Syk-Dependent reactive oxygen species production To trigger inflammasome assembly and restriction of parasite replication. *Journal of Immunology*, 199(6), 2055–2068. <https://doi.org/10.4049/jimmunol.1700258>

Luyao, S., Liwen, T., Yun, Ma, & Feng. (2017). Protection of flavonoids from smilax china L. rhizome on phenol mucilage-induced pelvic inflammation in rats by attenuating inflammation and fibrosis. *Journal of Functional Foods*.

Martinez, F. O., & Gordon, S. (2014). The M1 and M2 paradigm of macrophage activation: Time for reassessment. *F1000Prime Rep*, 6, 13. <https://doi.org/10.12703/p6-13>

Mitchell, C., & Prabhu, M. (2013). Pelvic inflammatory disease: Current concepts in pathogenesis, diagnosis and treatment. *Infectious Disease Clinics of North America*, 27 (4), 793–809. <https://doi.org/10.1016/j.idc.2013.08.004>

Nathan, C., & Ding, A. (2010). Nonresolving inflammation. *Cell*, 140(6), 871–882. <https://doi.org/10.1016/j.cell.2010.02.029>

Ornatowski, W., Lu, Q., Yegambaran, M., Garcia, A. E., Zemskov, E. A., Maltepe, E., ... Black, S. M. (2020). Complex interplay between autophagy and oxidative stress in the development of pulmonary disease. *Redox Biology*, 36, Article 101679. <https://doi.org/10.1016/j.redox.2020.101679>

Saitoh, T., & Akira, S. (2016). Regulation of inflammasomes by autophagy. *The Journal of Allergy and Clinical Immunology*, 138(1), 28–36. <https://doi.org/10.1016/j.jaci.2016.05.009>

Savaris, R. F., Fuhrich, D. G., Maissiat, J., Duarte, R. V., & Ross, J. (2020). Antibiotic therapy for pelvic inflammatory disease. *Cochrane Database of Systematic Reviews*, 8 (8), Cd010285. <https://doi.org/10.1002/14651858.CD010285.pub3>

Sevostyanova, O., Lisovskaya, T., Chistyakova, G., Kiseleva, M., Sevostyanova, N., Remizova, I., & Buev, Y. (2020). Proinflammatory mediators and reproductive failure in women with uterine fibroids. *Gynecological Endocrinology*, 36(sup1), 33–35. <https://doi.org/10.1080/09513590.2020.1816726>

Shapouri-Moghaddam, A., Mohammadian, S., Vaziri, H., Taghadosi, M., Esmaeili, S. A., Mardani, F., ... Sahebkar, A. (2018). Macrophage plasticity, polarization, and function in health and disease. *Journal of Cellular Physiology*, 233(9), 6425–6440. <https://doi.org/10.1002/jcp.26429>

Sharma, B. R., & Kanneganti, T. D. (2021). NLRP3 inflammasome in cancer and metabolic diseases. *Nature Immunology*, 22(5), 550–559. <https://doi.org/10.1038/s41590-021-00886-5>

Song, L., Tian, L., Ma, Y., Xie, Y., Feng, H., Qin, F., ... Wang, C. (2017). Protection of flavonoids from smilax china L. rhizome on phenol mucilage-induced pelvic inflammation in rats by attenuating inflammation and fibrosis. *Journal of Functional Foods*, 28, 194–204.

Tang, B., Wu, K., Meng, Q., & Wang, F. (2019). Comparison of the analgesic and Anti-Inflammatory effects of xiaoyuningkun decoction with cynanchum paniculatum and fukeqianjin in a mouse model of pelvic inflammatory disease. *Medical Science Monitor*, 25, 9094–9102. <https://doi.org/10.12659/msm.916070>

Tsukamoto, S., Kuma, A., Murakami, M., Kishi, C., Yamamoto, A., & Mizushima, N. (2008). Autophagy is essential for preimplantation development of mouse embryos. *Science*, 321(5885), 117–120. <https://doi.org/10.1126/science.1154822>

Wen, C., Gan, N., Zeng, T., Lv, M., Zhang, N., Zhou, H., ... Wang, X. (2020). Regulation of IL-10 gene expression by IL-6 via Stat3 in grass carp head kidney leucocytes. *Gene*, 741, Article 144579. <https://doi.org/10.1016/j.gene.2020.144579>

Zhang, X., He, M., Lei, S., Wu, B., Tan, T., Ouyang, H., ... Feng, Y. (2018a). An integrative investigation of the therapeutic mechanism of ainsliaea fragrans champ. in cervicitis using liquid chromatography tandem mass spectrometry based on a rat plasma metabolomics strategy. *Journal of Pharmaceutical and Biomedical Analysis*, 156, 221–231. <https://doi.org/10.1016/j.jpba.2018.04.048>

Zhang, X., Li, J., Xie, B., Wu, B., Lei, S., Yao, Y., ... Yang, S. (2018b). Comparative metabolomics analysis of cervicitis in human patients and a phenol Mucilage-Induced Rat model using liquid chromatography tandem mass spectrometry. *Frontiers in Pharmacology*, 9, 282. <https://doi.org/10.3389/fphar.2018.00282>

Zhang, Y., Li, W., Zou, L., Gong, Y., Zhang, P., Xing, S., & Yang, H. (2018c). Metabonomic study of the protective effect of fukeqianjin formula on multi-pathogen induced pelvic inflammatory disease in rats. *Chinese Medicine*, 13, 61. <https://doi.org/10.1186/s13020-018-0217-6>

Zhang, J., Liu, X., Wan, C., Liu, Y., Wang, Y., Meng, C., ... Jiang, C. (2020). NLRP3 inflammasome mediates M1 macrophage polarization and IL-1 β production in inflammatory root resorption. *Journal of Clinical Periodontology*, 47(4), 451–460. <https://doi.org/10.1111/jcpe.13258>

Zhang, Z., Zhang, C., & Zhang, S. (2022). Irisin activates M1 macrophage and suppresses Th2-Type immune response in rats with pelvic inflammatory disease. *Evidence-based Complementary and Alternative Medicine*, 2022, 5215915. <https://doi.org/10.1155/2022/5215915>

Zhang, L. J., Zhu, J. Y., Sun, M. Y., Song, Y. N., Rahman, K., Peng, C., ... Zhang, H. (2017). Anti-inflammatory effect of Man-Pen-Fang, a chinese herbal compound, on chronic pelvic inflammation in rats. *Journal of Ethnopharmacology*, 208, 57–65. <https://doi.org/10.1016/j.jep.2017.06.034>

Zou, W., Gong, L., Zhou, F., Long, Y., Li, Z., Xiao, Z., ... Liu, M. (2021). Anti-inflammatory effect of traditional chinese medicine preparation penyanling on pelvic inflammatory disease. *Journal of Ethnopharmacology*, 266, Article 113405. <https://doi.org/10.1016/j.jep.2020.113405>